Model Fitting and Validation: SIRS Model

Parameter Estimation, Uncertainty Quantification, and Bayesian Inference

AIMS Rwanda – Mathematical Modelling III

Rabecca, Honorine, Sylvestre, Samuel, Faida, Aline

February 13, 2026

INTRODUCTION

SIRS compartmental models describe how diseases spread by dividing a population into groups based on disease status. The SIRS model uses three compartments: Susceptible (S) people who are at a risk of getting disease; Infected (I) people currently sick and contagious; Recovered (R) people who have gained immunity. The "S" at the end means recovered people who eventually lost immunity and became susceptible again, making SIRS suitable for diseases like flu where reinfection occurs.

In our model, susceptible individuals became infected at a rate β through contact with infected individuals. Infected individuals recovered at a rate γ, while recovered individuals lost immunity and returned to the susceptible class at a rate ϕ. The parameter κ represented population changes due to births and deaths; however, in this model we assumed no population change and set $\kappa = 0$. With a total population size of $N = 100$, the ODE model used was given by:

$$\frac{dS}{dt} = \kappa N - \beta\frac{SI}{N} + \phi R - \kappa S, \quad \frac{dI}{dt} = \beta\frac{SI}{N} - \gamma I, \quad \frac{dR}{dt} = \gamma I - \phi R$$

METHODS

We solved the SIRS ODE (with $\kappa = 0$) to generate model trajectories, added Gaussian noise ($\sigma = 2$) to create 303 synthetic observations over $t \in [0, 50]$ days (using true parameter values $\beta = 0.5$, $\gamma = 0.2$, $\phi = 0.2$ and $(S_0, I_0, R_0) = (90, 10, 0)$), then fitted the key parameters (β, γ, ϕ) by least squares. We repeatedly resolved the ODE with `ode45` and used `fminsearch` to minimize the sum of squared errors between model outputs and the noisy data. After finding the best fit, we estimated the noise variance from the residuals, computed a numerical Jacobian to assess sensitivity and approximate parameter uncertainty, and then used these results as the starting point for MCMC to quantify full posterior uncertainty.

RESULTS

The results below summarize the SIRS model behaviour over time and how well it matches the noisy observations.

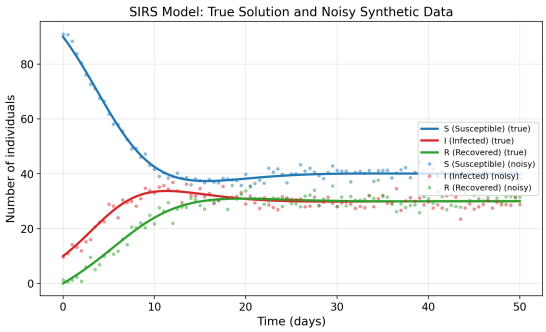

Figure 1: True SIRS curves and noisy observations (dots) for S, I, and R over time.

Figure 1 illustrates how the SIRS compartments change over time. The susceptible population drops rapidly as infection spreads, the infected population rises to a peak around day ∼10–12 and then drops a little, and the recovered population rises to about 30 by day ∼15–20 and then stays nearly constant. The dots are noisy observations obtained by adding Gaussian noise to the true model, so they scatter around each compartment.

Sensitivity to κ

Although $\kappa = 0$ was specified, we checked whether a small positive birth/death rate could fit the data better. We computed the sum of squares (SS) for κ values from 0 to 0.05 while keeping β, γ, ϕ at their true values.

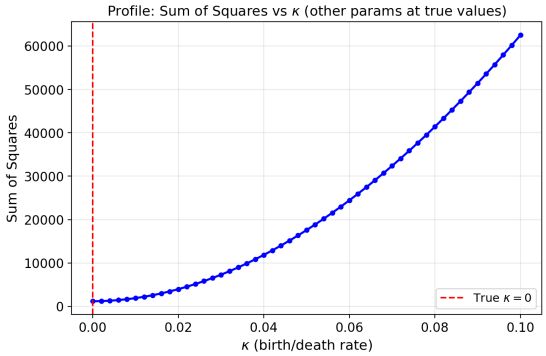

Figure 2: Sum of squares as a function of κ.

In Figure 2 the curve reaches its lowest point at exactly $\kappa = 0$ and rises consistently as κ increases. This tells us that the data is best explained with no births or deaths, so we can safely fix $\kappa = 0$.

Least Squares Estimation

We estimated the unknown parameters by finding the values that minimize the total squared difference between model predictions and noisy data ($\mathrm{SS}(\boldsymbol{\theta}) = \sum_{j,i}[y_i(t_j) - f_i(t_j;\boldsymbol{\theta})]^2$). We used MATLAB's `fminsearch` using initial guess $(0.4, 0.15, 0.15)$ and obtained: $\hat{\beta} = 0.4965$, $\hat{\gamma} = 0.1992$, $\hat{\phi} = 0.1940$. These estimates were close to the true values, indicating the parameters were well identified from the noisy data.

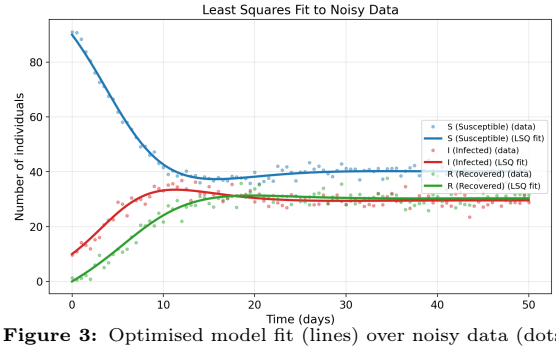

Figure 3: Optimised model fit (lines) over noisy data (dots)

In figure 3, the fitted curves pass through the centre of the noisy points for S, I, and R, showing the model follows the main data pattern well.

Jacobian-Based Uncertainty

To quantify uncertainty, the model was linearised around the LSQ optimum using the Jacobian matrix J. The parameter covariance was approximated by $C = \hat{\sigma}^2 \left(J^\top J\right)^{-1}$, with $\hat{\sigma}^2 = 3.80$ (true $= 4.0$) and $R^2 = 0.975$. The resulting correlation structure showed strong positive dependence, especially between β and γ ($r \approx 0.96$), meaning transmission

and recovery can trade off while still fitting the data well, ϕ was also strongly correlated with both (≈ 0.85).

The t-values were large above 3 ($t_\beta = 74.6$, $t_\gamma = 67.7$, $t_\phi = 51.2$), indicating all parameters were estimated with high statistical precision.

The fitted SIRS curves had a narrow 95% confidence band (low parameter uncertainty) and a wider 95% prediction band (including noise), most observed S, I, and R data points (black dots) lay within the prediction band, so the fitted curves and assumed noise level were consistent with the measurements as shown in Figure 4.

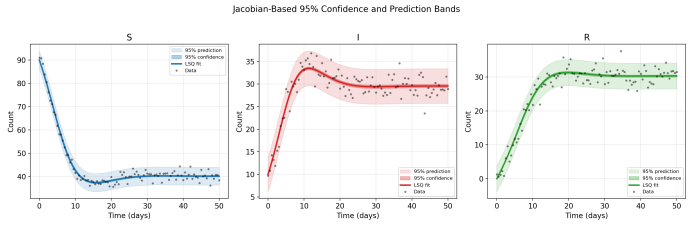

Figure 4: SIRS trajectories with 95% confidence and prediction bands

Bayesian Inference via MCMC

We used the DRAM sampler in the `mcmcstat` toolbox, starting at the least-squares estimate and using flat priors on $[0, 5]$. We ran 10,000 iterations, removed the first 25% as burn-in, and sampled σ^2 along with the parameters and the acceptance rate was 32%.

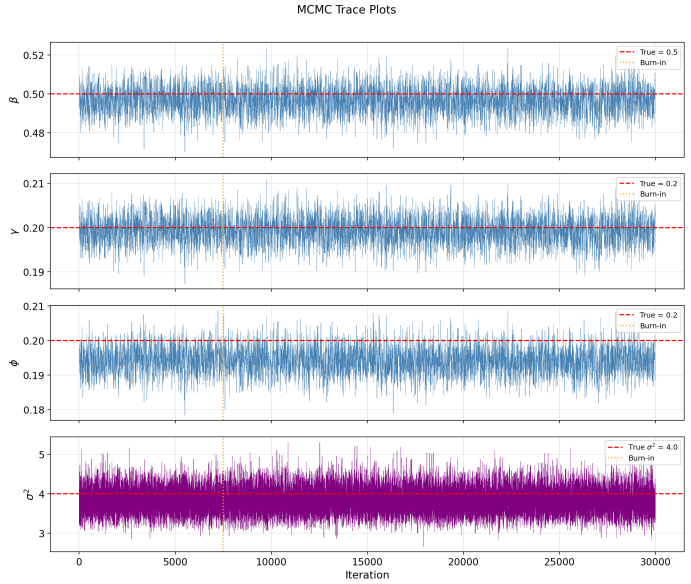

Figure 5: Trace plots for the MCMC samples of β, γ, ϕ, and σ^2.

Figure 5 shows that,after the burn-in period, the chains oscillated around parameter values with no visible trends, indicating good mixing and convergence of the MCMC sampler.

The autocorrelation dropped rapidly to near zero within about 15 lags for all parameters as seen in Figure 6 indicating weak dependence between samples.

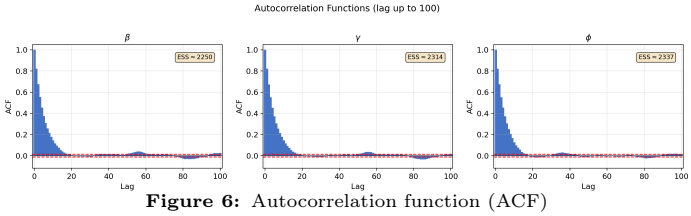

Figure 6: Autocorrelation function (ACF)

In summary, the MCMC estimated parameters and their 95% credible intervals were: β mean 0.497 with [0.484, 0.510], γ mean 0.199 with [0.193, 0.205], and ϕ mean 0.194 with [0.187, 0.202], the true values (0.500, 0.200, 0.200) all lie within these intervals.

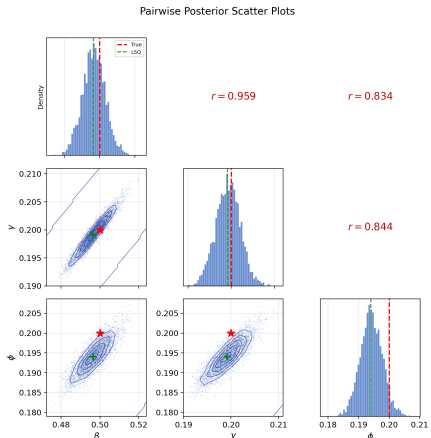

Figure 7: Pairwise posterior plots

From the above Figure 7 the diagonal histograms are the marginal posterior distributions, and the elongated off-diagonal clouds especially β–γ show strong positive posterior correlation, indicating weak separate identifiability.

Predictive Distribution and R_0

We sampled 500 parameter values from the posterior and solved the ODE each time to get a spread of possible trajectories. The predictive distribution fitted well, the median curves tracked the true trajectories and most points fell within the 95% interval, while the thin credible bands showed low uncertainty in the predicted S, I, and R paths as showed in graphs below.

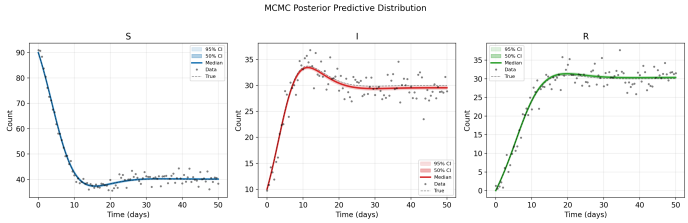

Figure 8: Posterior predictive distribution.

The posterior indicated that basic reproductive number, $R_0 = \beta/\gamma$ was about 2.49 (95% CI [2.47, 2.51]), close to the true 2.50 shown in Figure 9 below and therefore the disease would spread ($R_0 > 1$).

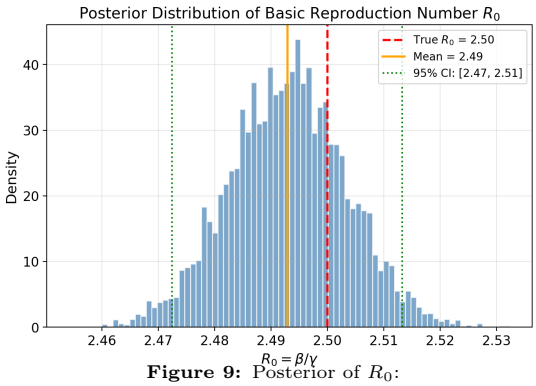

Figure 9: Posterior of R_0:

DISCUSSION

LSQ and MCMC produced very similar estimates and 95% intervals for (β, γ, ϕ), and the true parameter values lied within these ranges. The posterior showed a strong correlation between β and γ, meaning that changes in transmission could be adjusted by changes in recovery while still fitting the data well. Despite this correlation, the predictive intervals were narrow and covered most of the observed data. Diagnostic results indicated good MCMC mixing, supported $\kappa \approx 0$, and gave a posterior estimate of the basic reproduction number $R_0 = \beta/\gamma \approx 2.49$ ($[2.47, 2.51]$), providing strong evidence for sustained disease spread ($R_0 > 1$).